

See discussions, stats, and author profiles for this publication at: <https://www.researchgate.net/publication/5392815>

# Chiral Inversion of Gold Nanoparticles

ARTICLE *in* JOURNAL OF THE AMERICAN CHEMICAL SOCIETY · JULY 2008

Impact Factor: 12.11 · DOI: 10.1021/ja800256r · Source: PubMed

---

CITATIONS

99

---

READS

50

## 2 AUTHORS:



Cyrille Gautier

Université de Neuchâtel

15 PUBLICATIONS 610 CITATIONS

SEE PROFILE



Thomas Bürgi

University of Geneva

211 PUBLICATIONS 5,879 CITATIONS

SEE PROFILE

### Chiral Inversion of Gold Nanoparticles

Cyrille Gautier and Thomas Bürgi\*

Université de Neuchâtel, Institut de Microtechnique, Rue Emile-Argand 11,  
2009 Neuchâtel, Switzerland

Received January 15, 2008; E-mail: thomas.burgi@unine.ch

**Abstract:** The thiolate-for-thiolate ligand exchange was performed on well-defined gold nanoparticles under an inert atmosphere without any modification of the core size. This reaction is faster than the well-known core etching. Surprisingly, if a chiral thiol is exchanged for its opposite enantiomer, the optical activity in the metal-based electronic transitions is reversed although the form of the CD spectra remains largely unchanged. The extent of inversion corresponds to the overall ee of the chiral ligand in the system. This shows that the chiral arrangement of metal atoms in the metal particle (surface) can not withstand the driving force imposed by the ligand of opposite absolute configuration. If the incoming thiol has a different structure, the electronic transitions in the metal core are slightly modified whereas the absorption onset remains unchanged. These results emphasize the influence of the thiols on the structure of the gold nanoparticles and give insight on the ligand exchange pathways.

#### Introduction

The chirality of extended metal surfaces and of their nanometer size analogues, metallic nanoparticles (NPs), has become an emerging field of research in recent years triggered by potential applications in heterogeneous enantioselective catalysis,<sup>1,2</sup> enantiodiscrimination,<sup>3</sup> enantioseparation, enantioselective crystallization,<sup>4,5</sup> liquid crystal displays,<sup>6</sup> and nonlinear optics. On the one hand, bare high Miller index metal surfaces such as Ag(643) are naturally and intrinsically chiral. The chirality of these surfaces is associated with kinked steps. Similarly, density functional theory (DFT) calculations have shown that small naked metallic NPs can also be intrinsically chiral.<sup>7–9</sup> On the other hand, the adsorption of a chiral or even an achiral/prochiral molecule (the modifier) on a surface can break reflection symmetry of both the molecule and the surface and thus strengthens the asymmetry of a chiral surface or imparts chirality onto an achiral surface. This phenomenon is the first basic manifestation of chirality at surfaces. One modifier can have different ionic forms and conformations,<sup>10</sup> which can lead to different expressions of local chirality. The different chiral motifs can furthermore self-assemble at the nano- or at the

microscale in a single phase or in a cascade of chiral or achiral phases. The adsorption of an achiral/prochiral compound can lead to a racemic mixture of domains with opposite chirality,<sup>11–13</sup> whereas the adsorption of a chiral compound can create a local handedness, which is sustained over the entire surface.<sup>14,15</sup> Of course, this global organization is dictated by a balance of molecule–molecule interactions such as hydrogen bonds,  $\pi$  stacking, van der Waals forces, charge-transfer and dipole–dipole interactions, and molecule–metal interactions such as thiol–, amine–, carboxylate–, and phosphine–metal interactions. In addition, the adsorption of a modifier can distort the structure of extended metal surfaces.<sup>11,15</sup> For example, the adsorption of (*R,R*)-tartaric acid on Ni(110) goes along with a local relaxation of the metal surface atoms.<sup>15</sup> This chiral stress imparted on the surface upon adsorption of a molecule is known as a chiral footprint. Chirality transfer through metal interactions represents a key parameter for the propagation of the local chirality to the macroscale, as has been proposed for the chiral organization of (*R,R*)-bitartrate molecules in long chains on the Cu(110) surface.<sup>14</sup>

Gold NPs in the nanometer-size range covered by enantiopure chiral thiols or phosphines such as L-glutathione (GSH)<sup>16–19</sup> as well as the two enantiomers of penicillamine,<sup>20</sup> *N*-isobutryl-

- (1) Bönemann, H.; Braun, G. A. *Angew. Chem., Int. Ed.* **1996**, *35*, 1992–1995.
- (2) Studer, M.; Blaser, H. U.; Exner, C. *Adv. Synth. Catal.* **2003**, *345*, 45–65.
- (3) Bieri, M.; Gautier, C.; Bürgi, T. *Chem. Phys. Phys. Chem.* **2007**, *9*, 671–685.
- (4) David, H.; Dressler, Y. M. *Chirality* **2007**, *19*, 358–365.
- (5) Dressler, D. H.; Mastai, Y. J. *Colloid Interface Sci.* **2007**, *310*, 653–660.
- (6) Qi, H.; Hegmann, T. J. *Mater. Chem.* **2006**, *16*, 4197–4205.
- (7) Wetzel, T. L.; DePristo, A. E. *J. Chem. Phys.* **1996**, *105*, 572–580.
- (8) Garzón, I. L.; Beltrán, M. R.; Gonzalez, G.; Gutierrez-Gonzalez, I.; Michaelian, K.; Reyes-Nava, J. A.; Rodriguez-Hernandez, J. I. *Eur. Phys. J. D* **2003**, *24*, 105–109.
- (9) Garzón, I. L.; Reyes-Nava, J. A.; Rodríguez-Hernández, J. I.; Sigal, I.; Beltrán, M. R.; Michaelian, K. *Phys. Rev. B* **2002**, *66*, 073403.
- (10) Barlow, S. M.; Raval, R. *Curr. Opin. Colloid Interface Sci.* **2007**, *13*, 65–73.

- (11) Schunack, M.; Lægsgaard, E.; Stensgaard, I.; Johannsen, I.; Besenbacher, F. *Angew. Chem., Int. Ed.* **2001**, *40*, 2623–2626.
- (12) Viswanathan, R.; Zasadzinski, J. A.; Schwartz, D. K. *Nature* **1994**, *368*, 440–443.
- (13) Lopinski, G. P.; Moffatt, D. J.; Wayner, D. D. M.; Wolkow, R. A. *Nature* **1998**, *392*, 909.
- (14) Ortega Lorenzo, M.; Baddeley, C. J.; Muryn, C.; Raval, R. *Nature* **2000**, *404*, 376–379.
- (15) Humblot, V.; Haq, S.; Muryn, C.; Hofer, W. A.; Raval, R. *J. Am. Chem. Soc.* **2002**, *124*, 503–510.
- (16) Negishi, Y.; Nobusada, K.; Tsukuda, T. *J. Am. Chem. Soc.* **2005**, *127*, 5261–5270.
- (17) Negishi, Y.; Takasugi, Y.; Sato, S.; Yao, H.; Kimura, K.; Tsukuda, T. *J. Am. Chem. Soc.* **2004**, *126*, 6518–6519.
- (18) Schaaff, T. G.; Knight, G.; Shafgullin, M. N.; Borkman, R. F.; Whetten, R. L. *J. Phys. Chem. B* **1998**, *102*, 10643–10646.

cysteine (NIC),<sup>21</sup> 2,2'-bis(diphenylphosphino)-1,1'-biphenyl (BINAP),<sup>23</sup> and 1,1'-binaphthyl-2,2'-dithiol (BINAS)<sup>24</sup> exhibit optical activity in metal-based electronic transitions (MBET), which shows that the electronic structure of the gold particle is chiral. The findings reported so far for optically active NPs can be summarized as follows: Optical activity differs with the size of the NPs and generally decreases as the size is increasing. As for classical chiral molecules, the circular dichroism (CD) spectra of NPs display a mirror image relationship when covered with the two opposite enantiomers and no optical activity is observed when a racemic mixture of ligand is used. A common feature of the modifiers inducing CD signals reported up to now is that they contain several functional groups able to coordinate to the gold particle.<sup>21,25</sup>

Interestingly, calculations have indicated that the optical activity in the MBET can arise from an intrinsically chiral gold core<sup>8,9</sup> as well as from an achiral one if the latter is placed in a chiral environment. The latter possibility includes the chiral arrangement of the ligands and the influence of the stereocenter of the chiral ligands (through space or through bonds) on the electronic structure of the metal. For example, it has been predicted recently by using a dissymmetrically perturbed particle-in-a-box model that CD signals can arise from chiral adsorbates on symmetric particles.<sup>26</sup> These two different origins of optical activity can act concurrently, but their own contribution remained to be determined. Very recently an intermediate model corresponding to the local chiral distortion of the surface atoms involved in the adsorption of the ligand (similar to a chiral footprint) was evidenced for NPs composed of 102 gold atoms and 44 *p*-mercaptobenzoic acid (*p*-MBA) molecules. Note that the *p*-MBA ligand is achiral. Indeed, the first total structure determination by X-ray crystallography of a small gold–thiolate NP was recently accomplished by Jadzinsky et al.<sup>27</sup> Each NP is chiral, and the crystal is composed of a racemic mixture of both enantiomers. The gold atoms in the core of the NPs are packed in a symmetric Marks decahedron (MD) structure, which is very similar to the fcc structure of bulk gold. The chirality of the overall particle arises at two levels. First, the adsorbate forms dimers on the NP surface connected through a gold atom that is somewhat detached from the gold core.<sup>27,28</sup> In these structures the sulfur atoms represent chiral centers. It should be noted that each enantiomer of the NPs possesses a small enantiomeric excess (ee) in the absolute configuration of the adsorbed *p*-MBA. Second, chirality also arises from the arrangement of equatorial gold atoms on the surface of the gold NPs. The asymmetric structure of the surface of the NPs reflects the interaction with the prochiral thiol. This important X-ray study confirms the theoretical prediction that, upon adsorption, an achiral compound not only decorates the surface of the NPs

but also distorts locally the structure of the surface.<sup>29</sup> Furthermore, the local distortion may be comparable to some extent to the chiral footprint observed on extended metal surfaces.

It is likely that similar structural motifs, as the ones elucidated by the X-ray study mentioned above, are also found for the small gold particles<sup>29</sup> exhibiting optical activity in MBET, although the latter consist much less than 102 gold atoms and therefore the achiral core, if existing at all, would be very small. Evidently the chiral arrangement of surface gold atoms plays a major role for the optical activity of the NPs. Covering the latter by one enantiomer of a chiral ligand may favor one chiral motif on the surface over its enantiomer, and this transfer of chirality from the adsorbate to the metal particle (surface) is favored by multiple adsorbate–particle interactions. However, the behavior of this chiral distortion has not been studied yet. A key question remains whether the chiral arrangement of the metal surface atoms is stable enough to withstand a ligand exchange reaction. This would, for example, allow the fine-tuning of a surface in view of its use in heterogeneous asymmetric catalysis. One could also imagine that the chiral imprint left by the outgoing ligand can influence the adsorption of a prochiral incoming ligand. Indeed, DFT calculations have predicted a difference of ~100 meV in the adsorption energy of the right-handed and the left-handed enantiomers of cysteine on a Au<sub>55</sub> cluster.<sup>30</sup>

Here we investigate the behavior of small monodisperse NPs, containing ten to a few tens of gold atoms only, covered with one enantiomer when exposed to the free thiol of the opposite absolute configuration, to a racemic mixture of thiols and to an achiral thiol under an inert atmosphere. The retention of the core size and the evolution of the absorption in UV–vis and of the optical activity in the MBET are followed by electrophoresis and UV–vis and CD spectroscopy, respectively. The results give new insight into the chiral properties of these particles and furthermore provide information on thiolate-for-thiolate ligand exchange reactions.

## Results and Discussion

**Effect of Dissolved Oxygen on Core-Size Retention during the Thiolate-for-Thiolate Ligand Exchange.** The first set of experiments was performed with the gold NPs covered by either *N*-isobutyl-L-cysteine (NILC) or *N*-isobutyl-D-cysteine (NIDC, Chart 1). These particles were separated by polyacrylamide gel electrophoresis (PAGE) into eight well-defined compounds, i.e., compounds with a precise number of gold atoms and ligands.<sup>21</sup> Separated NPs were referred to as compounds **1–8** (see Figure 1 A) according to their electrophoretic mobility with the yellowish compound **2** being the second most mobile species. In a previous report,<sup>21</sup> it was shown that the UV–vis spectra are strikingly similar for analogous compounds **1–3** covered by NIC and GSH.<sup>16</sup> This comparison allowed us to assign the three smallest compounds **1**, **2**, and **3** to Au<sub>10</sub>(NIC)<sub>10</sub>, Au<sub>15</sub>–(NIC)<sub>13</sub>, and Au<sub>18</sub>(NIC)<sub>14</sub>, respectively. The NPs covered with *N*-acetyl-L-cysteine (NALC) also contain the species **1–3** (see later). The isolated and dialyzed compounds could be stored for weeks without noticeable degradation, as verified by PAGE and UV–vis spectroscopy.

We noticed a pronounced effect of dissolved oxygen on the evolution of the CD signals of the gold particles upon addition of further thiol. Figure 2A shows CD spectra recorded after

(19) Schaaff, T. G.; Whetten, R. L. *J. Phys. Chem. B* **2000**, *104*, 2630–2641.

(20) Yao, H.; Miki, K.; Nishida, N.; Sasaki, A.; Kimura, K. *J. Am. Chem. Soc.* **2005**, *127*, 15536–15543.

(21) Gautier, C.; Bürgi, T. *J. Am. Chem. Soc.* **2006**, *128*, 11079–11087.

(22) Tamura, M.; Fujihara, H. *J. Am. Chem. Soc.* **2003**, *125*, 15742–15743.

(23) Yanagimoto, Y.; Negishi, Y.; Fujihara, H.; Tsukuda, T. *J. Phys. Chem. B* **2006**, *110*, 11611–11614.

(24) Gautier, C.; Taras, R.; Gladiali, S.; Bürgi, T. *Chirality* **2008**, *20*, 486–493.

(25) Gautier, C.; Bürgi, T. *Chem. Commun.* **2005**, *43*, 5393–5395.

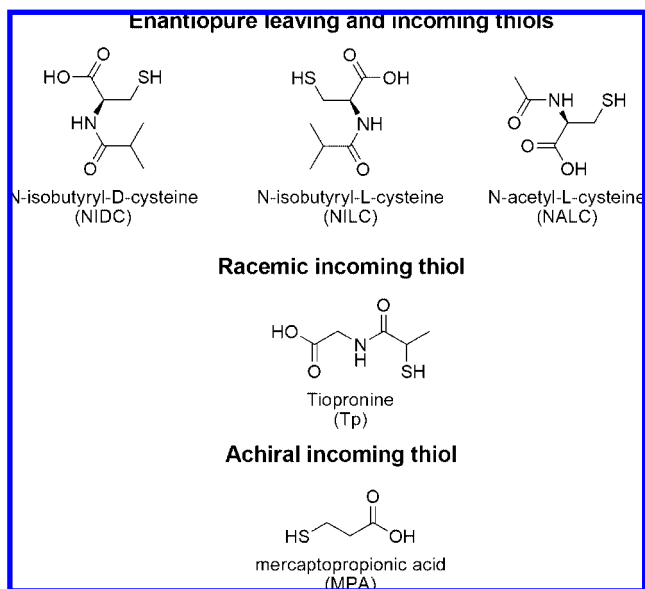
(26) Goldsmith, M. R.; George, C. B.; Zuber, G.; Naaman, R.; Waldeck, D. H.; Wipf, P.; Beratan, D. N. *Phys. Chem. Chem. Phys.* **2006**, *8*, 63–67.

(27) Jadzinsky, P. D.; Calero, G.; Ackerson, C. J.; Bushnell, D. A.; Kornberg, R. D. *Science* **2007**, *318*, 430–433.

(28) Whetten, R. L.; Price, R. C. *Science* **2007**, *318*, 407–408.

(29) Häkkinen, H.; Walter, M.; Gronbeck, H. *J. Phys. Chem. B* **2006**, *110*, 9927–9931.

(30) López-Lozano, X.; Pérez, L. A.; Garzón, I. L. *Phys. Rev. Lett.* **2006**, *97*, 233401.

**Chart 1.** Chemical Structures of the Thiols Used

addition of NIDC to **2** ( $\text{Au}_{15}(\text{NILC})_{13}$ ) under aerobic condition, whereas Figure 2B shows the evolution of the optical activity after addition of NILC to  $\text{Au}_{15}(\text{NIDC})_{13}$  under inert conditions. Note that for these experiments the ratio between added thiol and thiol adsorbed on the initial particles was 9. In both cases the signals at 420 and 336 nm were quickly inverted during the first 20 min to an extent of 56% under aerobic conditions (C) and 70% under an inert atmosphere (D). At 336 nm, the optical activity is not reversed (reduced to 44%) under aerobic conditions whereas it is reversed at 82% under an inert atmosphere. The shape of the full CD spectra is more preserved under an inert atmosphere. The larger differences in terms of shape (difference of inversion at 336 and 420 nm) for the spectra under aerobic conditions might be explained by the formation of particles of different sizes and by the appearance of Au(I) thiolate species (*vide infra*). Indeed, in the presence of oxygen the signals subsequently decreased with time and the solution

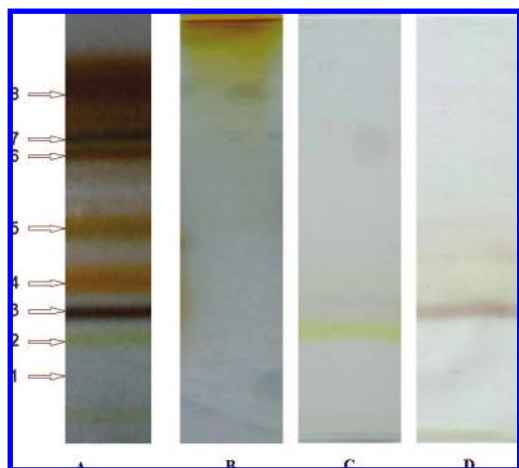


**Figure 1.** PAGE separation of NPs protected with NIC after synthesis (A). The separated compounds are numbered from 1–8 according to their decreasing electrophoretic mobility. The smallest compound 1 is only visible under UV irradiation. Isolation of compound 2,  $\text{Au}_{15}(\text{NIC})_{13}$ , after reaction with the opposite enantiomer in PBS under aerobic condition (B) and under inert atmosphere (C). Isolation of compound 3,  $\text{Au}_{18}(\text{NILC})_{14}$ , after reaction with NIDC under inert atmosphere (D).

was no more optically active after less than 1 h, whereas the signal was stable in the absence of oxygen.

The size distribution after exchange was monitored by PAGE. For the experiment under aerobic conditions compound **2** was not observed by PAGE and the sample showed a drastic reduction of electrophoretic mobility after 1 day (see Figure 1B). The batch under an inert atmosphere was rapidly quenched by removing the excess of free thiols and phosphate buffered saline (PBS) buffer by ultrafiltration (UF). PAGE (see Figure 1C) showed almost exclusively compound **2** with the minor presence of the larger compounds **3**–**5**. A similar behavior was observed for the same type of reaction on compound **3** with the discrete appearance of the adjacent species **2** and **4**, which are very similar in terms of size (Figure 1D). It should be noted that UF was not performed rigorously under an inert atmosphere and thus some influence of oxygen on the size distribution observed in Figure 1C, D is possible even for the reaction under anaerobic conditions. The intensity of the inverted signals in Figure 2B is smaller (70% of optical inversion) than the one that could be expected from the ee of NIC in the system (80%), which is probably due to the formation of larger particles, as evidenced by PAGE (Figure 1 C). The larger compounds **3**–**5** have considerably smaller anisotropy factors,<sup>21</sup> and thus the CD spectrum is dominated by compound **2** ( $\text{Au}_{15}(\text{NIDC})_{13}$ ).

#### Inversion of the Absolute Configuration of the Ligands.

Further experiments were performed under an inert atmosphere with the species **2** and **3** of the gold NPs protected with NILC, which correspond, respectively, to  $\text{Au}_{15}(\text{NILC})_{13}$  and  $\text{Au}_{18}(\text{NILC})_{14}$ . These compounds can be isolated again after 1 h of reaction with the ligand of opposite absolute configuration by UF and PAGE in order to eliminate the small contribution of NPs of different sizes. The ratio between NIDC (incoming) and NILC (outgoing) enantiomers is 9 for these two experiments. Figure 1 shows that the electrophoretic mobility of **2** (C) and **3** (D) are not modified after the reaction with NIDC. In addition, Figure 3A shows that both UV–vis spectra of the isolated NPs **2** and **3** after an exchange reaction with NIDC remain unchanged. This confirms that the size and the total number of ligands are preserved during the reaction, in agreement with electrophoresis. More interestingly, the CD spectra are reversed with a quasi-perfect mirror image relationship. The signals are blue-shifted by 1 to 2 nm after exchange, and the ratio of the signals at 360 and 420 nm is slightly different (see Figure 3B). The anisotropy factor,  $\Delta\epsilon/\epsilon$ , shows that the optical activity is reversed at 78% (at 360 nm) for the reaction of  $\text{Au}_{15}(\text{NILC})_{13}$  with NIDC (see Figure 3C). This percentage of inversion, about 80% (magnitude of the inverted signal is 80% of the initial signal), corresponds very well to the overall ee of NIC in the system (added NIDC plus NILC adsorbed on the NPs). The observations are similar for the reaction on **3**  $\text{Au}_{18}(\text{NILC})_{14}$ . Due to the weaker optical activity the relatively large noise prevents accurate quantification. However, it is evident that the form of the CD spectrum does not change drastically upon inversion for these two compounds **2** and **3**.

The observed inversion of the CD signal indicates rapid ligand exchange and has interesting implications on the nature of the chirality of the gold particles. The fact that the shapes of the CD spectra are unchanged and that their intensity corresponds to the overall ee of the ligand in the system is an argument against the model which attributes the optical activity in MBET to a symmetric core perturbed by a dissymmetric or chiral field. In fact, Beratan et al.<sup>26</sup> have shown that the computed chiroptical response changes significantly when the chiral field is modified.



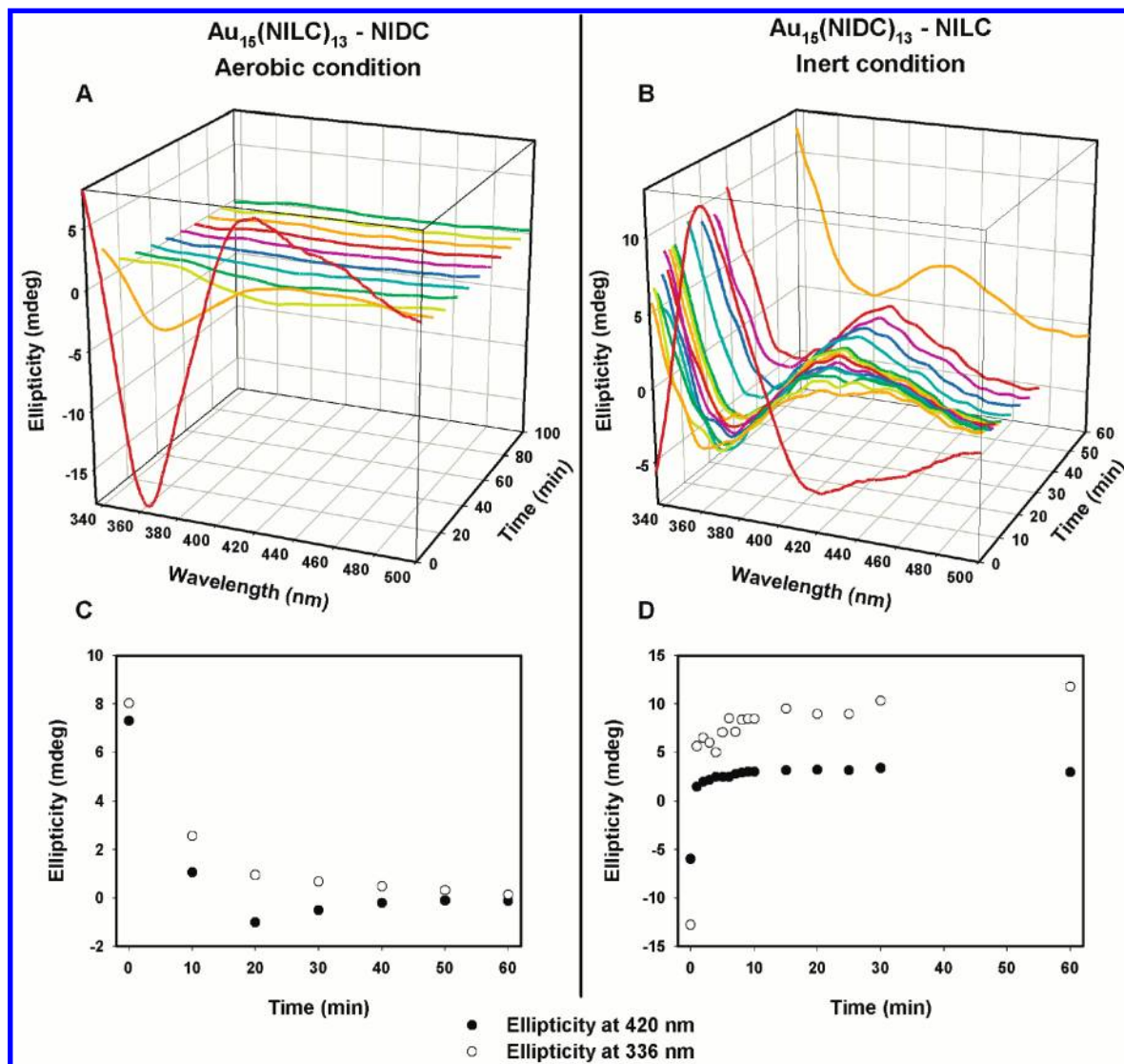


**Figure 2.** Time evolution of CD spectra after addition of 14.7 mg of NIDC (A) or 11 mg of NILC (B) to 3 mL of PBS pH 7.4 containing, respectively, 3.6 mg of  $\text{Au}_{15}(\text{NILC})_{13}$  under aerobic condition and 2.7 mg of  $\text{Au}_{15}(\text{NIDC})_{13}$  under inert atmosphere. Time evolution of the ellipticity at 420 nm (●) and 336 nm (○) during the ligand exchange reaction:  $\text{Au}_{15}(\text{NILC})_{13}$ -NIDC under aerobic condition (C) and  $\text{Au}_{15}(\text{NIDC})_{13}$ -NILC under inert atmosphere (D).

Similarly, it is well-known that the chiroptical response of a transition metal ion changes when the ligand sphere, i.e., the chiral field, is changing.<sup>31,32</sup> The latter is influenced by the number and arrangement of point charges (charged functional groups of NIC). The chiral field changes under our conditions where one to two ligands per particle have the opposite absolute configuration (assuming a statistical distribution of NIC enantiomers on the particles). Therefore the findings in Figure 3 contradict a model based mainly on the chiral arrangement of the thiols on an achiral metal core. The other proposed model is based on the assumption that the core of small metal particles can adopt intrinsically chiral structures.<sup>9</sup> If such particles grow in the presence of a passivating chiral enantiopure thiol, then one enantiomeric form of the chiral core could be stabilized over the other, which would explain the observed optical activity in the MBET. One could then imagine that this enantiomeric form of the metal core is prevented, even if the thiol ligand is

exchanged for example by the opposite enantiomer. The observed inversion of the optical activity for species **2** and **3** shows that this is not the case. Hence, the metal core, if it is intrinsically chiral, relaxes to the other enantiomer, when the absolute configuration of the ligand is changed. In other words, still under the assumption of an intrinsically chiral metal core, the barrier between the two enantiomeric forms of the metal core is too small compared to the driving force imposed on it by the change in absolute configuration of the thiol ligand. Assuming an analogous structure as the one reported by Jadzinsky et al. it seems clear that the chiral local distortion of the gold atoms involved in the adsorption of the chiral thiol (e.g., “chiral footprint”) is the key parameter for the optical activity in the MBET. The findings reported here thus show that this chiral footprint does not support a ligand exchange reaction and the incoming chiral thiol finally imposes its own chiral footprint. This implies that the resolution of a racemic mixture of NPs might not be possible using derivatization with a chiral thiol.

**Exchange with a Racemic Mixture of Chiral Thiol or with an Achiral Thiol.** These experiments are performed under an

(31) Höhn, E. G.; Weigang, O. E. *J. Chem. Phys.* **1968**, *48*, 1127–1137.  
(32) Yasui, T.; Hidaka, J.; Shimura, Y. *Bull. Chem. Soc. Jpn.* **1966**, *39*, 2417–2424.

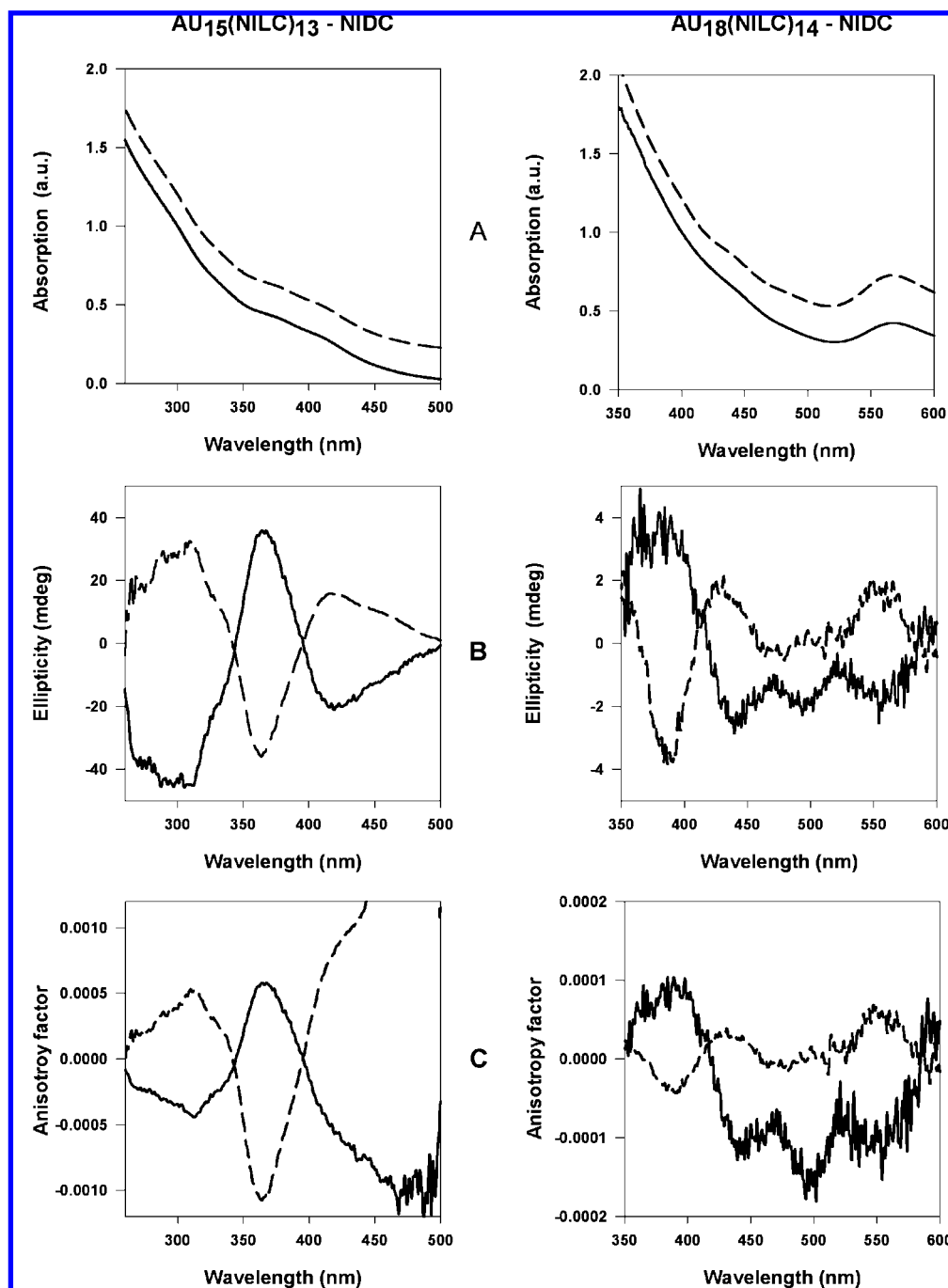


**Figure 3.** UV-vis spectra normalized at 300 nm and offset for clarity (A), CD spectra (B), and anisotropy factor (C) of  $\text{Au}_{15}(\text{NILC})_{13}$  (left) and  $\text{Au}_{18}(\text{NILC})_{14}$  (right) before (dashed line) and after ligand exchange reaction with NIDC (solid line). UV-vis spectra of  $\text{Au}_{15}(\text{NILC})_{13}$  and  $\text{Au}_{18}(\text{NILC})_{14}$  are offset and normalized to one in absorbance at 300 and 400 nm, respectively, and CD spectra of  $\text{Au}_{15}(\text{NILC})_{13}$  are normalized to 35.8 mdeg at 364 nm for clarity.

inert atmosphere with  $\text{Au}_{15}(\text{NALC})_{13}$  in the presence of either a racemic mixture of tiopronin (Tp) or the achiral 3-mercaptopropionic acid (MPA) with the molar ratio between the incoming ligands and NALC limited to 4. The former reaction leads to a large diminution of the optical activity and a qualitative change of the CD spectra, whereas the latter annihilates completely the CD signal (see Supporting Information for the evolution of optical activity with time). The size evolution is monitored by PAGE. Figure 4 compares the results of PAGE for the crude gold NPs protected with either NALC (A) or Tp (B) as well as the size evolution of  $\text{Au}_{15}(\text{NALC})_{13}$  (2) upon exchange with the Tp (C) and the MPA (D). The ligand

exchange reaction with Tp leads to two main species which do not correspond to the isolated species for the crude gold NPs protected with either the NALC or with the Tp. However, the electrophoretic mobility of the products and of the starting material are quite similar. Furthermore, Tp and NALC have similar chemical formulas and the same charges (see Chart 1). This implies that the resulting NPs might be very similar in size despite their different colors. The situation is similar for the exchange reaction involving MPA. In this case three distinct fractions are isolated. The most mobile fraction is yellow as the starting NALC NPs **2** but has a higher electrophoretic mobility probably due to the smaller size of the incoming MPA.

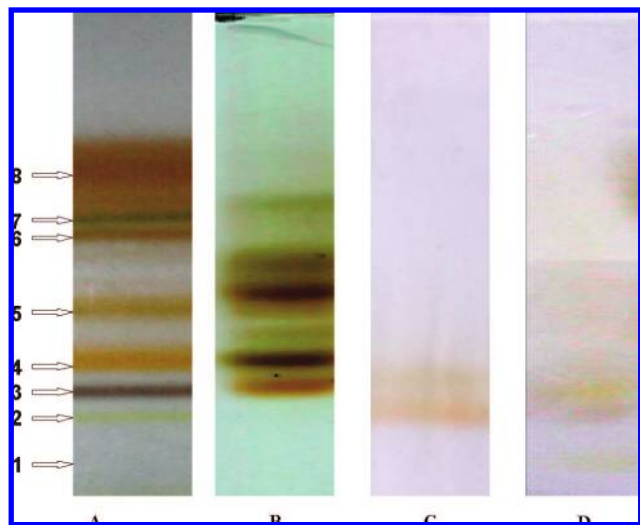


**Figure 4.** PAGE separation of NPs protected with NALC (A) and racemic Tp (B) after syntheses. Separation of compound **2** ( $\text{Au}_{15}(\text{NALC})_{13}$ ) after reaction with racemic Tp (C) and MPA (D) in PBS pH 7.4 under inert atmosphere.

The two species resulting from the ligand exchange with Tp were furthermore isolated in order to control their size and their individual optical activity. Figure 5 shows the UV–vis (right) and CD (left) spectra of the two isolated fractions. The UV–vis spectra of the products and of **2** are different in terms of shape, but the absorption onsets are very similar for the three species ( $\sim 700$  nm). This implies that the sizes of these compounds are very close<sup>33</sup> and that the variation of the electronic structure may not be attributed to a variation of the size but rather to a difference in the surface structure (i.e., footprint). The optical activity is very weak for the two species and may still be attributed to the nonexchanged NALC rather than due to enantioselective adsorption.<sup>30</sup> These findings emphasize once more the flexibility of the NPs structure and the effect of the adsorbates onto the electronic structure of the cluster. For example, NALC and NILC have been shown to have the same type of adsorption on gold NPs by VCD (vibrational circular dichroism) and DFT calculations.<sup>21,25</sup> Corresponding fractions of NPs separated by PAGE show similar UV–vis spectra.

It has been debated in literature whether the optical activity displayed by small metal particles is an inherent property or caused by a ligand-induced reconstruction.<sup>8,9,19–24,34–36</sup> Our results, obtained by CD spectroscopy on size-selected NPs after ligand exchange, clearly indicate the importance of the ligand. Independent of the model, i.e., whether the metal core is intrinsically chiral or whether the chirality is associated with the surface region of the metal particle only, the exchange reactions clearly show that the absolute configuration is not easily retained. This indicates that small gold particles covered with thiolates are rather fluxional. On the one hand this means that chirality is straightforwardly imposed on them, by an appropriate chiral thiol ligand. On the other hand the chiral

structure is easily lost again or changed by removing or exchanging the ligand.

**Insight on the Thiolate-for-Thiolate Ligand Exchange.** These experiments further contain interesting information about thiolate-for-thiolate ligand exchange in subnanometer particles and the different evolutions of the core size in the presence of excess thiol under an inert atmosphere or in aerobic conditions. Ligand exchange reactions on gold NPs have been extensively used to create new functionalized NPs. The thiolate-for-thiolate ligand exchange reaction has been studied with a wide variety of spectroscopic tools such as gas chromatography (GC),<sup>37</sup> nuclear magnetic resonance (NMR),<sup>38–41</sup> thermogravimetric analysis (TGA), X-ray photoelectron spectroscopy (XPS),<sup>42</sup> cyclic voltammetry (CV),<sup>38</sup> differential pulse voltammetry (DPV),<sup>40</sup> fluorescence spectroscopy,<sup>43,44</sup> transmission electron microscopy (TEM), and electron paramagnetic resonance (EPR).<sup>45,46</sup> These studies have given precious indications on the kinetic of the exchange, on the substituent effects (electronic and steric),<sup>39</sup> on the core charge effects,<sup>40</sup> and finally on the mechanism of the ligand exchange reaction. To date, kinetics studies have concluded that the ligand exchange process is associative ( $\text{S}_{\text{N}}2$ -like),<sup>41,47</sup> dissociative ( $\text{S}_{\text{N}}1$ -like),<sup>40,45,46</sup> or a combination thereof mediated by an oxidized form of gold such as Au(I) thiolate species.<sup>48</sup> However, almost all these studies were carried on particles with a more or less pronounced size distribution. So far, the reports dealing with the core size evolution during ligand exchange are not in complete agreement. On the one hand some reports, mainly relying on TEM, indicate that thiolate-for-thiolate ligand replacements on Au NPs lead to retention of the Au core size.<sup>49–51</sup> On the other hand, Murray et al.<sup>52</sup> have recently demonstrated by mass spectrometry that reaction of  $\text{Au}_{55}(\text{PPh}_3)_{12}\text{Cl}_6$  with hexanethiol under argon yields  $\text{Au}_{75}$  clusters. In the same manner, Tsukuda and Teranishi<sup>53</sup> reported recently the large scale synthesis of thiolated  $\text{Au}_{25}$  cluster under a  $\text{N}_2$  atmosphere via ligand exchange reaction with phosphine-stabilized  $\text{Au}_{11}$  clusters as starting material. They also suggested that the population of the smaller particles decreased after aeration. The two latter studies deal with a phosphine-for-thiol exchange reaction. This may differ from the thiolate-for-

- (37) Kassam, A.; Bremner, G.; Clark, B.; Ulibarri, G.; Lennox, R. B. *J. Am. Chem. Soc.* **2006**, *128*, 3476–3477.
- (38) Hostetler, M. J.; Green, S. J.; Stokes, J. J.; Murray, R. W. *J. Am. Chem. Soc.* **1996**, *118*, 4212–4213.
- (39) Donkers, R. L.; Song, Y.; Murray, R. W. *Langmuir* **2004**, *20*, 4703–4707.
- (40) Song, Y.; Murray, R. W. *J. Am. Chem. Soc.* **2002**, *124*, 7096–7102.
- (41) Hostetler, M. J.; Templeton, A. C.; Murray, R. W. *Langmuir* **1999**, *15*, 3782–3789.
- (42) Woehle, G. H.; Brown, L. O.; Hutchison, J. E. *J. Am. Chem. Soc.* **2005**, *127*, 2172–2183.
- (43) Montalti, M.; Prodi, L.; Zaccaroni, N.; Baxter, R.; Teobaldi, G.; Zerbetto, F. *J. Am. Chem. Soc.* **2003**, *125*, 5172–5174.
- (44) Nerambourg, N.; Werts, M. H. V.; Charlot, M.; Blanchard-Desce, M. *Langmuir* **2007**, *23*, 5563–5570.
- (45) Ionita, P.; Caragheorghopol, A.; Gilbert, B. C.; Chechik, V. *J. Am. Chem. Soc.* **2002**, *124*, 9048–9049.
- (46) Ionita, P.; Caragheorghopol, A.; Gilbert, B. C.; Chechik, V. *Langmuir* **2004**, *20*, 11536–11544.
- (47) Montalti, M.; Prodi, L.; Zaccaroni, N.; Baxter, R.; Teobaldi, G.; Zerbetto, F. *Langmuir* **2003**, *19*, 5172–5174.
- (48) Song, Y.; Huang, T.; Murray, R. W. *J. Am. Chem. Soc.* **2003**, *125*, 11694–11701.
- (49) Woehle, G. H.; Warner, M. G.; Hutchison, J. E. *J. Phys. Chem. B* **2002**, *106*, 9979–9981.
- (50) Woehle, G. H.; Hutchison, J. E. *Inorg. Chem.* **2005**, *44*, 6149–6158.
- (51) Yang, Y.; Chen, S. *Nano Lett.* **2003**, *3*, 75–79.
- (52) Balasubramanian, R.; Guo, R.; Mills, A. J.; Murray, R. W. *J. Am. Chem. Soc.* **2005**, *127*, 8126–8132.
- (53) Shichibu, Y.; Negishi, Y.; Tsukuda, T.; Teranishi, T. *J. Am. Chem. Soc.* **2005**, *127*, 13464–13465.

- (33) Wyrwas, R. B.; Alvarez, M. M.; Khoury, J. T.; Price, R. C.; Schaaff, T. G.; Whetten, R. L. *Eur. Phys. J. D* **2007**, *43*, 91–95.
- (34) Li, T.; Park, H. G.; Lee, H. S.; Choi, S. H. *Nanotechnology* **2004**, *15*, S660–S663.
- (35) Shemer, G.; Krichevski, O.; Markovich, G.; Molotsky, T.; Lubitz, I.; Kotlyar, A. B. *J. Am. Chem. Soc.* **2006**, *128*, 11006–11007.
- (36) Yao, H.; Fukui, T.; Kimura, K. *J. Phys. Chem. C* **2007**, *111*, 14968–14976.

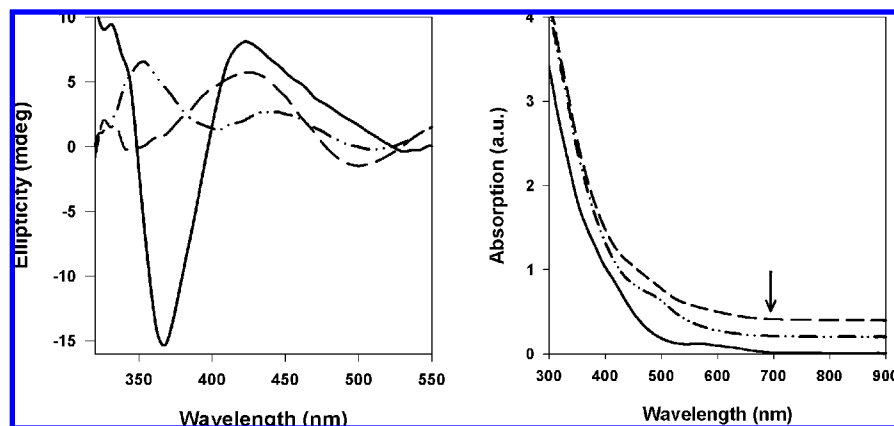


**Figure 5.** CD (left) and UV-vis (right) spectra of the species isolated by PAGE after the reaction of  $\text{Au}_{15}(\text{NALC})_{13}$  with Tp. The spectra of  $\text{Au}_{15}(\text{NALC})_{13}$  before reaction, the most mobile, and the second isolated fraction correspond, respectively, to the solid, the dash point, and the dash lines. CD spectra of the two products isolated after the reaction are multiplied by a factor 5, and UV-vis spectra are normalized at 400 nm and offset for clarity. The vertical arrow indicates the absorption onset for the three UV-vis spectra.

thiolate exchange studied here, but in both cases the exchange was done in the presence of an excess of incoming thiol. Tsukuda and Teranishi have recently demonstrated the extremely high stability of the  $\text{Au}_{25}(\text{SG})_{18}$  clusters against core etching in the presence of a large excess of GSH even in aerobic conditions.<sup>54</sup> This study demonstrates that, in aerobic conditions, the glutathionate protected clusters smaller than  $\text{Au}_{25}$  are etched into Au(I) thiolate polymers and very small clusters, whereas the bigger clusters are converted to  $\text{Au}_{25}$  by etching. Here we take advantage of the charge and of the solubility of our NPs in water to achieve size separation of the NPs with molecular precision using PAGE. Furthermore the exchange of one enantiomer of a chiral thiol on the surface of a well-defined cluster for its enantiomer is probably one of the most straightforward systems to study a thiolate-for-thiolate exchange reaction because the incoming and the outgoing thiols only differ by their absolute configuration. As a result the size evolution and the total content of ligand are easily probed by UV-vis spectroscopy and electrophoretic mobility, whereas the kinetics is followed by CD spectroscopy. As discussed above, for both  $\text{Au}_{15}(\text{NILC})_{13}$  and  $\text{Au}_{18}(\text{NILC})_{14}$ , the present study provides strong evidence that the size memory can be kept to a large extent during the ligand exchange reaction under an inert atmosphere. The CD measurements also demonstrate that this reaction is very fast. The mechanism of thiolate-for-thiolate ligand exchange is not established, but Murray et al.<sup>48</sup> have shown that the exchange is inhibited when conducted under  $\text{N}_2$  and in the absence of Au(I) thiolate species. Their results imply participation of an oxidized form of Au probably in the form of Au(I) thiolate. Some of these Au(I) thiolates and especially ringlike units have been predicted by DFT calculations<sup>29,55,56</sup> and have been observed by electrospray mass spectrometry<sup>16,17,57</sup> and might be a general structural motif of very small clusters composed of 10 to 50 gold atoms which is the size range of the NPs studied here. The X-ray study of Jadzinsky has brought to light that for slightly bigger NPs (102 gold atoms) the Au(I) thiolate motif is present but mainly in the form of dimers.<sup>27</sup> These predicted building blocks could also play a significant role

for the relatively fast kinetic of the described exchanges and for the optical activity in the MBET described before. According to Figure 2B and D, the reaction in the absence of  $\text{O}_2$  and without a Au(I) thiolate catalyst was almost complete in  $\sim 5$  min, whereas ligand exchange on gold particles takes a few hours according to published work.<sup>48</sup> Furthermore, we observed that, even under aerobic conditions, the optical activity is reversed within 20 min without a drastic modification of the signal (see Figure 2A and C). However, after that the CD spectra progressively decreased and its shape was modified. This implies that two different processes are involved. On the one hand, the first process involves ligand exchange without modification of the size of the clusters. This very fast ligand exchange without alteration of the core size can be explained for example by a radical mechanism, which does not involve Au(I) thiolate leaving groups and which has been evidenced by the spin trapping technique.<sup>58</sup> On the other hand, the second process, the core etching, is slower, catalyzed by  $\text{O}_2$ , and leads to a modification of the size distribution probably by the formation of Au(I) thiolate polymers. Interestingly, the yield of the ligand exchange reaction in the absence of oxygen (first process) calculated from the anisotropy factor (Figure 3 C) is close to the ee of the ligand in the system, which indicates a dynamic equilibrium constant ( $K_{\text{eq}}$ ) close to unity. This was already observed by GC in thiolate-for-thiolate exchange reactions when the incoming and outgoing ligands were chemically very similar.<sup>37</sup> This would mean that adsorption and desorption are reversible and that the two enantiomers of NIC have similar affinities for the NPs.

## Conclusions

In conclusion, the thiolate-for-thiolate ligand exchange under inert condition can be performed on nanoclusters without degradation of the core size. The optical activity in the MBET of small monodisperse gold particles covered by one enantiomer of NIC is reversed when exposed to the opposite enantiomer. This shows that the optical activity is dictated by the chiral thiol. If the particles exhibit an intrinsically chiral structure, the results furthermore imply that this structure is not stable enough in one of its enantiomeric forms to withstand a switch of the absolute

(54) Shichibu, Y.; Negishi, Y.; Tsunoyama, H.; Kanehara, M.; Teranishi, T.; Tsukuda, T. *Small* **2007**, *3*, 835–839.

(55) Grönbeck, H.; Walter, M.; Häkkinen, H. *J. Am. Chem. Soc.* **2006**, *128*, 10268–10275.

(56) Iwasa, T.; Nobusada, K. *J. Phys. Chem. C* **2007**, *111*, 45–49.

(57) Gies, A. P.; Hercules, D. M.; Gerdon, A. E.; Cliffl, D. E. *J. Am. Chem. Soc.* **2007**, *129*, 1095–1104.

(58) Ionita, P.; Gilbert, B. C.; Chechik, V. *Angew. Chem., Int. Ed.* **2005**, *44*, 3720–3722.



configuration of the passivating thiol. This observation reveals the influence of the adsorbed thiols on the structure of the cluster surface and demonstrates its key role in the optical activity. The extent of ligand exchange of NILC for its opposite enantiomer corresponds to the ee of overall NIC in the system. When the incoming thiol is different from the leaving one, the electronic structure of the cluster can be slightly different even if the size of the resulting clusters is similar. This shows the influence of the nature of the thiols on the electronic structure of the cluster.

**Acknowledgment.** Financial support by the Swiss National Science Foundation is kindly acknowledged.

**Supporting Information Available:** Experimental section: Materials and procedures. Time evolution of CD signals after addition of tiopronin and 3-mercaptopropionic acid to  $\text{Au}_{15}(\text{NALC})_{13}$ . This information is available free of charge via the Internet at <http://pubs.acs.org>.

JA800256R